Moderate High Power 1 to 20 µs and kHz Ho:YAG Thin Disk Laser Pulses for Laser Lithotripsy

Günther Renz
Institute of Technical Physics, German Aerospace Center
Deutsches Zentrum für Luft- und Raumfahrt, Pfaffenwaldring 38, 70569 Stuttgart

ABSTRACT

An acousto-optically or self-oscillation pulsed thin disk Ho:YAG laser system at 2.1 µm with an average power in the 10 W range will be presented for laser lithotripsy. In the case of cw operation the thin disk Ho:YAG is either pumped with InP diode stacks or with a thulium fiber laser which leads to a laser output power of 20 W at an optical-to-optical efficiency of 30%. For the gain switched mode of operation a modulated Tm-fiber laser is used to produce self-oscillation pulses. A favored pulse lengths for uric acid stone ablation is known to be at a few µs pulse duration which can be delivered by the thin disk laser technology. In the state of the art laser lithotripter, stone material is typically ablated with 250 to 750 µs pulses at 5 to 10 Hz and with pulse energies up to a few Joule. The ablation mechanism is performed in this case by vaporization into stone dust and fragmentation. With the thin disk laser technology, 1 to 20 µs-laser pulses with a repetition rate of a few kHz and with pulse energies in the mJ-range are available. The ablation mechanism is in this case due to a local heating of the stone material with a decomposition of the crystalline structure into calcium carbonate powder which can be handled by the human body. As a joint process to this thermal effect, imploding water vapor bubbles between the fiber end and the stone material produce sporadic shock waves which help clear out the stone dust and biological material.

Keywords: thin disk laser, Ho:YAG, laser lithotripsy

1. INTRODUCTION

Thulium fiber laser pumping or direct InP diode pumping of rare-earth active Holmium in YAG in connection with multi-pass pumping thin disk laser concepts leads to power scalable laser systems in the 2 µm 'eye-save' wavelength region which is proposed to be used for intra corporeal lithotripsy in medical applications. Holmium with a wavelength of 2.1 µm shows good water absorption characteristics and is therefore a preferred laser material for these applications [1, 2]. The various commercially available Ho:YAG rod laser systems utilize pulses with a pulse length in the order of 500 µs, pulse energies close to 1 J and are run at repetition rates of up to multiple 10 Hz at average output powers between 20 and 30 W [3, 4]. Using a cw thulium fiber laser for urinary stones ablation resulted in a strongly fragmentation of the material [5]. A high-energy Ho:YAG rod oscillator system gives pulses of a few 100 ns which are too short for these applications [6]. In contrast, the Ho:YAG thin disk laser system produces pulses of a few microsecond with pulse energies of a few milli-Joule and repetition rates in the kHz-range and will be investigated for laser lithotripsy.

1.1 Ho:YAG thin disk laser system

In figure 1 the schematic of the thin disk laser system is depicted. The Ho:YAG thin disk is pumped with a 24 pump pass module (Dausinger + Giesen GmbH) [7, 8]. The Ho:YAG thin disk has a thickness of 300 µm and a diameter of 12 mm and is soldered onto a copper heat sink which is water cooled. The resonator with a length of 20 cm consists on one side of the highly reflecting back side of the thin disk and on the other side of an output coupler with an optimized transmission of 0.3% and a radius of curvature of 100 cm. The Ho:YAG thin disk laser is pumped with a 1.908 µm single mode Tm fiber laser (IPG Photonics) or with a stack of InP diode lasers (QPC Laser). In the case of the single mode Tm fiber laser, the laser beam is transferred through a 600 µm multimode fiber before it enters the thin disk module. With the Tm fiber laser pumping the pump spot diameter on the 2.5% Ho:YAG thin disk is 2 mm which can be seen in the CCD camera picture of figure 1. For a power of 100 W of the Tm fiber laser the power density on the disk is 3 kW/cm^2.

disk diameter: 12 mm

pump spot: 2 mm

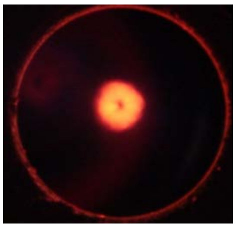

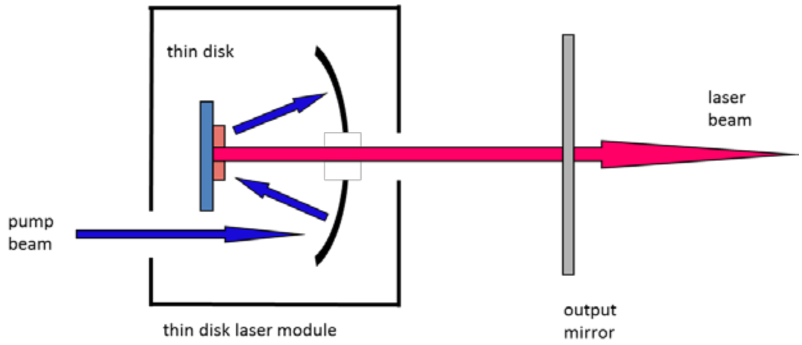

Figure 1. Schematic of thin disk laser configuration with picture of the pump spot on the disk.

In figure 2 the cw oscillator output power is shown for the InP diode stack pumping scheme. An output power of more than 20 W with an optical-to-optical efficiency of almost 30% has been reached.

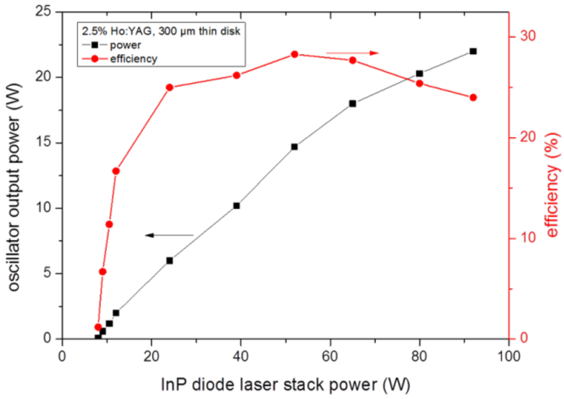

Figure 2. Cw Ho:YAG laser power and efficiency versus InP diode stack pump power.

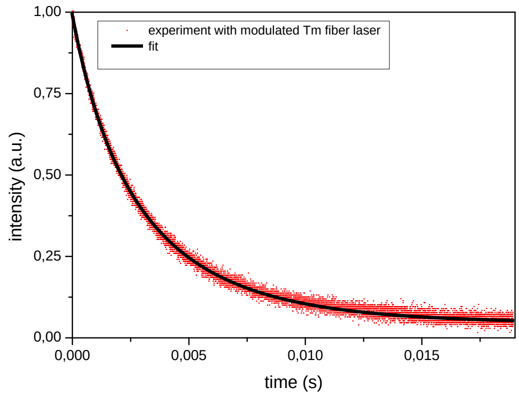

Figure 3. Ho^{3+} lifetime measurement and fit with inclusion of up-conversion processes at 0.1 kW/cm^2 (3% of saturation).

For higher output couplings than 0.3% the output power is reduced. This shows that there are additional losses in the laser system. Therefore, the Ho:YAG laser material will be investigated in the next paragraph concerning internal losses.

1.2 Ho:YAG laser material parameters

In figure 3 a Ho^{3+} lifetime measurement for a 300 µm thin 2.5% Ho:YAG disk is depicted. The pumping of the laser material has been performed with a modulated Tm fiber laser which operates in the kHz-range at an average power of a few Watt. It is known, that in a Ho^{3+} laser material, Ho:Ho up-conversion processes through neighbor atoms out of the $^5I_7$ manifold to higher $^5I_5$ energy levels lead to additional losses [9, 10, 11]. The lifetime of the $^5I_5$ manifold is known to be short (~1 µs) because of non-radiative relaxation and reduces therefore the lifetime of the upper laser level. The exponential fit curve to the emitted photon intensity, P_7, results for a 2.5% Ho in YAG (saturation of $3.5\cdot10^{20}$ atoms/cm^3) to a lifetime of the upper laser level of τ_7 = 4.5 ms. The Ho:Ho up-conversion, covered by the P_{77} parameter, results in a fit parameter of N_{70} of $6\cdot10^{-18}$ cm^3/s with N_{70} the population density at the end of the pump pulse after Barnes:

$$P_7 = N_{70} \cdot \exp(-\frac{t}{\tau_7})/\{1 + P_{77} \cdot \tau_7 \cdot N_{70} \cdot \left[1 - \exp\left(-\frac{t}{\tau_7}\right)\right]\} \quad (1)$$

For higher pump power densities the lifetime stays relatively constant until starting at a tenfold pump power density, the lifetime increases which shows that the single fit model is not applicable anymore.

In a thin disk laser resonator design the output coupling is typically low. For a Ho:YAG thin disk laser resonator design with one disk the optimal output coupling is in the order of 1%. Since Ho:Ho up-conversion losses limit the output efficiency of the laser, any additional losses in the resonator, coming for instance from an acousto-optical (AOM) or electro-optical switch material, will further reduce the efficiency of the thin disk laser system in the order of 50%. An alternative to an actively switched laser system is therefore a gain switched system where the pump laser is modulated and the self-oscillation mechanism is used to produce the laser pulses with a much higher efficiency. In the following section an AOM-pulsed and a self-oscillation pulsed Ho:YAG thin disk laser system will be investigated concerning applicability for laser lithotripsy.

1.3 Acousto-optically pulsed or self-oscillation pulsed Ho:YAG thin disk laser systems

In figure 4 the output laser pulse signals and the trigger signals are depicted for a AOM-switched (left) and a self-oscillation pulsed (right) Ho:YAG laser system.

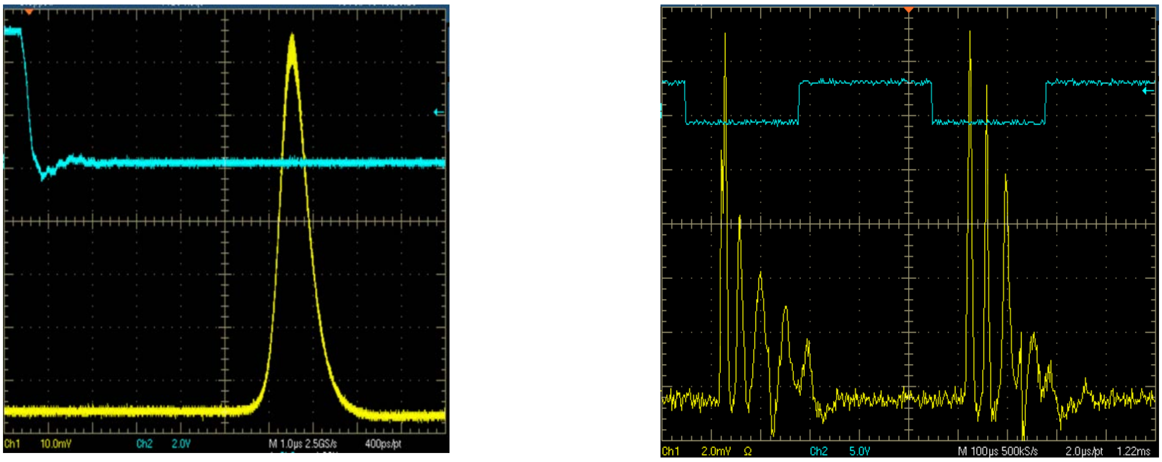

Figure 4. AOM pulsed 1 µs laser signal (left) and self-oscillation pulses of 5 to 20 µs (right) with trigger pulses in the upper traces.

In figure 5 the numerical solution of the rate equations for a 4-level system is shown with the inversion and the laser intensity versus the time in cavity lifetime [12]. A sequence of multiple laser pulses with increasing pulse durations in the order of 10 µs can be seen.

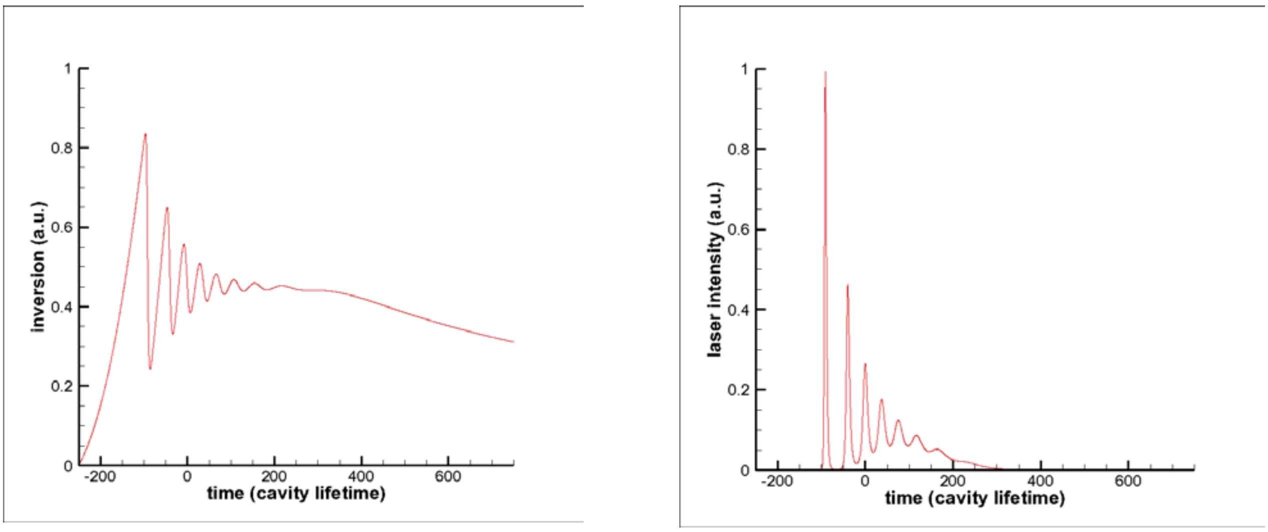

Figure 5. Simulated self-oscillation signal: inversion (left) and laser intensity (right).

In figure 6 the thin disk oscillator output power is shown for a cw and for a kHz-modulated Tm fiber laser pump excitation. With a duty cycle of up to 90% for the kHz-modulated case the power level of the cw case can almost be reached with an optical-to-optical efficiency of up to 30%. Scaling the laser system to higher output power is only limited by the recently available Tm fiber laser pump power in our laboratory of 50 W but with two 100 W Tm fiber lasers coupled into a thin disk module, 40 W output power can be expected.

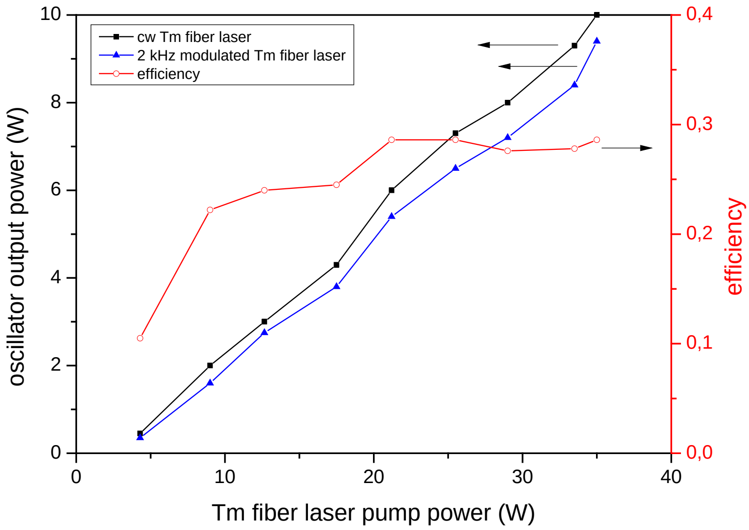

Figure 6. Cw and pulsed oscillator output power and efficiency versus Tm fiber laser pump power.

The laser output mode has been measured with a pyro-electric camera (Pyrocam, 100x100 µm pixel sizes) and is depicted in figure 7 (left) to be multimode. The simulated result of the laser output beam is shown in figure 7 (right). In the numerical simulation the wave equation in the slowly varying amplitude approximation is solved with a split-step FFT method. The multimode output beam with highest output power is reached by a slightly misaligned thin disk module and resonator. In the experiment the measurement shows an oval mode pattern which can be simulated by an astigmatism. The beam quality measurement in the horizontal and vertical direction gives an M^2 of 3 and 7, respectively. This output laser beam, focused with a lens of 10 cm focus length, shows a focus dimension of 400 by 600 µm which is suitable to be transferred into a 600 µm fiber for medical applications. For smaller fiber diameters the beam quality has be improved.

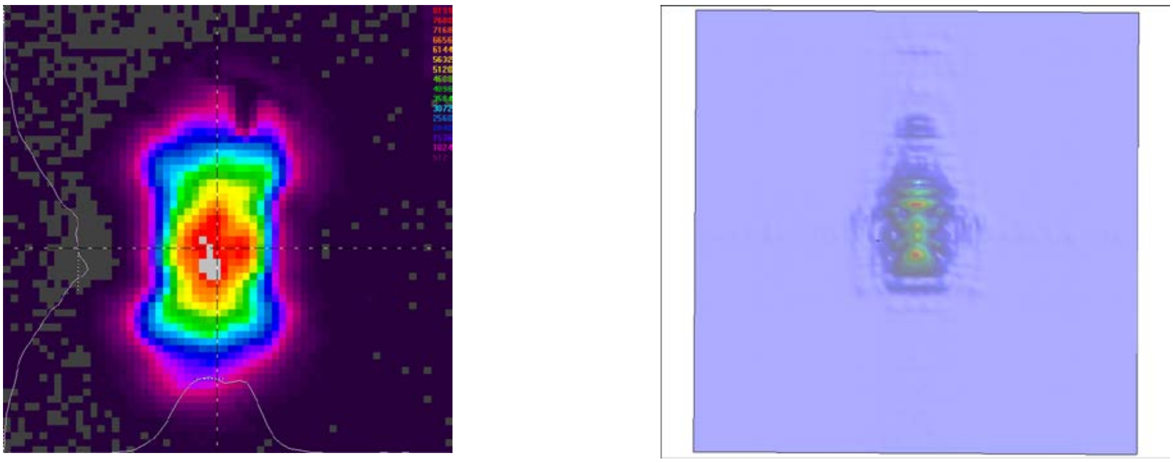

Figure 7. Experimental laser output beam (left) and simulated results with a high astigmatism (right).

For an exactly aligned thin disk module the measured laser beam profile is shown in figure 8 (left) to be closer to a rotationally symmetric beam profile but with a low output power of a few Watt and efficiency compared to the multimode case.

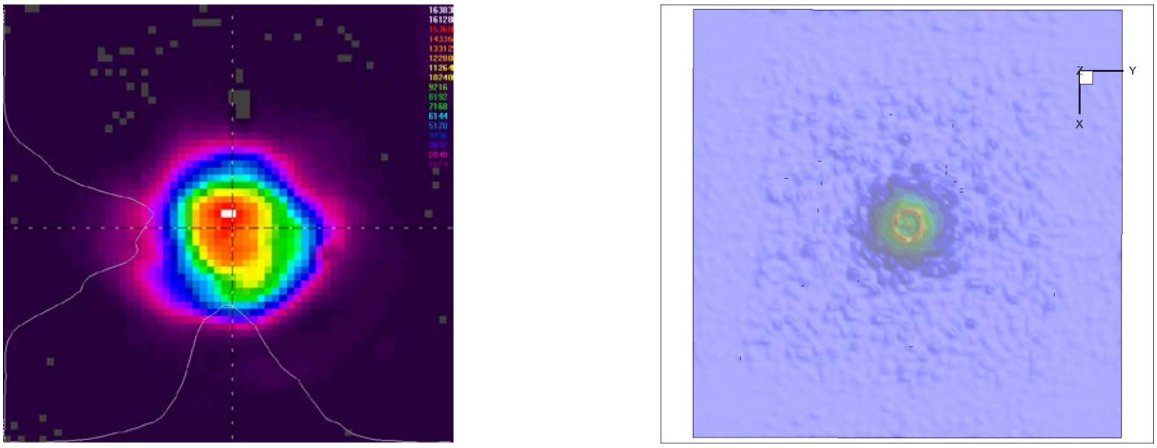

Figure 8. Measured beam profile for a low output power (left) and simulation with a low astigmatism (right).

1.4 Medical application of pulsed Ho:YAG thin disk laser systems

In urology, the most used clinical laser procedure is the laser lithotripsy where urinary, biliary and salivary calculi (stones) are fragmented. The most popular laser material for a laser lithotripter is Ho:YAG at 2.1 µm in a rod type configuration. The typical laser parameters are 250 to 750 µs pulses at 5 to 10 Hz and with pulse energies up to a few Joule. The laser energy is absorbed in water at this wavelength in 0.5 mm making it concerning the wavelength an ideal surgical laser tool. Using either an AOM- or a self-oscillation pulsed Ho:YAG thin disk laser, it is possible to operate the laser lithotripter with pulse durations of a few microseconds and repetition rates in the kHz-range with an average laser power in the order of 10 W.

At the start-up of the laser ablation process the fiber position was adjusted to touch with its end the stone. The stone itself was immersed into water. By touching the stone with the fiber tip, the highest ablation rates were measured. Using the Ho:YAG thin disk laser in the cw operational mode resulted in an ablation crater of the stone material but at the same time the stone cracked and fragmented into large pieces.

In figure 9 (left) the end of the 600 µm fiber is depicted with a water vapor bubble of approximately 1 mm of diameter.

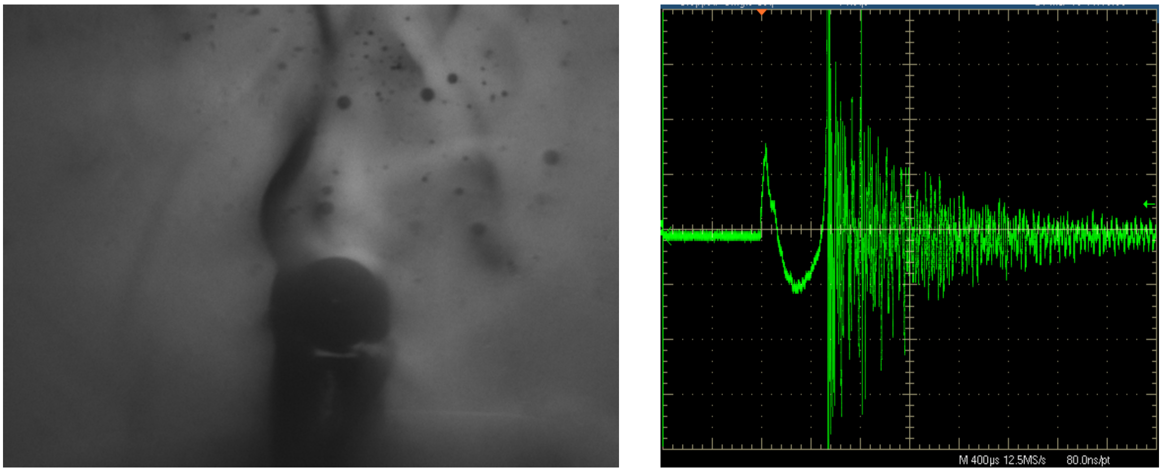

Figure 9. CCD camera picture of water vapor bubble just before implosion (left) and pressure transducer measurement of imploding water vapor bubble (right).

The bubble is attached to the fiber tip and is created by the heated water due to the absorbed laser power. During the water vapor bubble collapse the bubble experiences an attracting force (Bjerknes force) towards the rigid boundary which can be the surface of a nearby stone material. At the end of the implosion a shock wave leaves the interaction zone. On the picture of figure 9 (left), smaller bubbles can be seen which are from previously created bubbles. The collapsed water vapor bubble creates a cracking noise which can be detected with a pressure sensor (PCB Piezotronics, resolution 2 µs) roughly 1 cm apart from the bubble (see figure 9 (right)). The first single peak is created by the collapsed bubble and lasts for about 100 µs. At the end of the signal, multiple reflections from the surroundings can be seen.

In figure 10 the normalized water bubble radius (r/r_{max}) with r_{max} ~ 1 mm from figure 9 (left) versus the normalized implosion time (t/t_0) with t_0 ~ 100 µs from figure 9 (right) is shown, calculated with the analytical integration formular after the classical Lord Rayleigh model from 1917:

$$\frac{t}{t_0} = 1.34 \cdot \int_{r_{max}}^{1} \frac{dr}{\sqrt{\frac{1}{r^3}-1}} \tag{2}$$

Rayleigh analyzed the collapse of an empty spherical cavity with a constant pressure difference. It can be seen in figure 10, that at the end of the collapse period there is a rapid implosion instability which produces the shock wave.

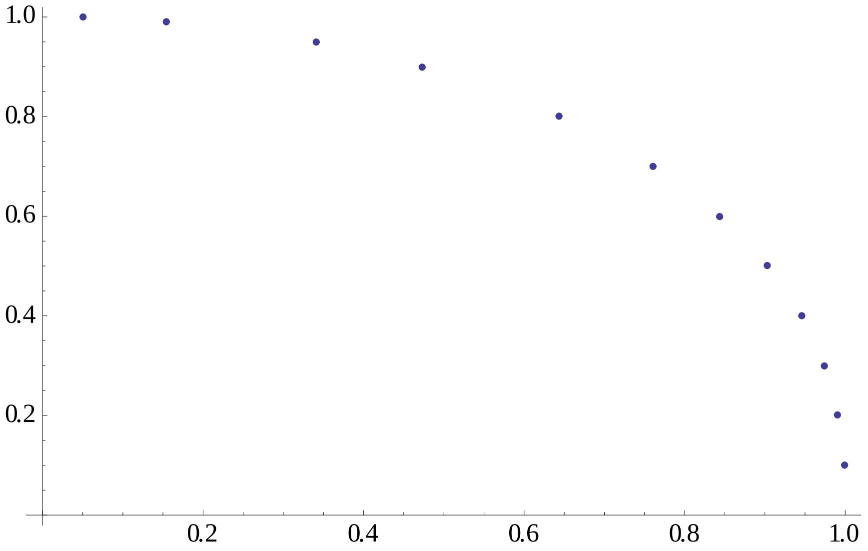

Figure 10. Normalized water vapor bubble radius (r/r_{max}) versus normalized implosion time (t/t_0) in dimensionless Rayleigh coordinates.

The pulse energy of the µs-pulses is in the order of 1 mJ and is applied to the uric acid stone to locally heat up the stone material. Above a temperature of approximately 100°C, the water in the calcium oxalate monohydrate crystal ($CaC_2O_4*H_2O$) starts to be dehydrated, leading to a reduction of the crystal mass of approximately 12% (see figure 11). For temperatures above 400°C, the crystal structure starts to be decomposed into calcium carbonate powder ($CaCO_3$) with a mass reduction of approximately 18% under production of carbon dioxide. For even higher temperatures above 600°C calcium carbonate decomposes into calcium monoxide and carbon dioxide [13].

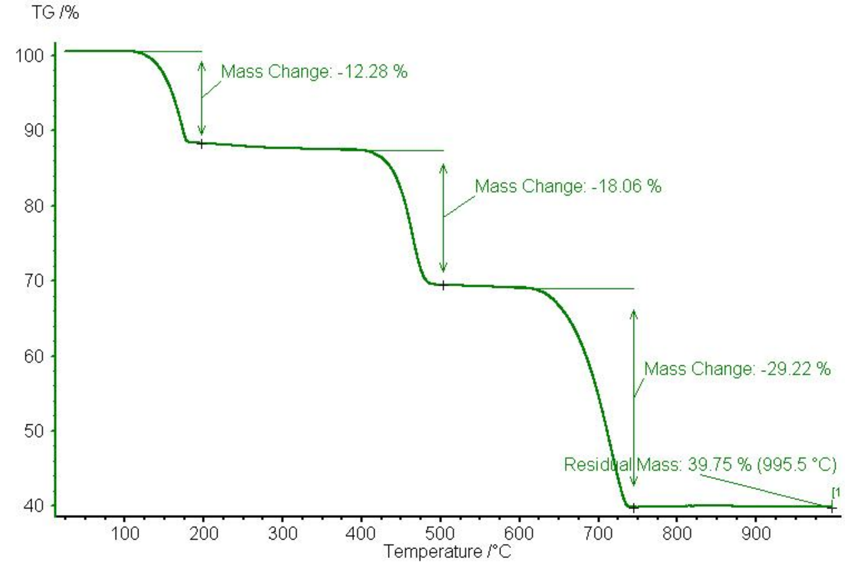

Figure 11. Temperature dependent decomposition of calcium oxalate monohydrate crystal ($CaC_2O_4*H_2O$) from [Fernando Vallejos-Burgos, http://en.wikipedia.org/wiki/File:Whewellite_tga.jpg].

In figure 12 (left), the laser ablated artificial stone material is depicted. The diameter of the laser ablated crater is roughly 1 mm. On the outer rim of the crater, the structure of the multimode laser field coming out of the 600 µm fiber can be recognized by multiple holes in a circular configuration. In figure 12 (right), a microscopic picture of a ablated crater shows the single calcium oxalate monohydrate crystals of sizes between 10 and 100 µm embedded into a biological material. The stone ablation reached 1 mg/(W·min) with a laser average power of a few Watt. In future work, a scaled Ho:YAG thin disk laser system will be developed. With one or two Tm fiber lasers with a pump power of up to 200 W a self-oscillation pulsed laser power on the surface of the stone material of 10 to 20 W can be expected. With this novel laser lithotripter local thermal decomposition of the stone material in combination with the formation of shock waves should give access to a more safely and optimized laser lithotripsy.

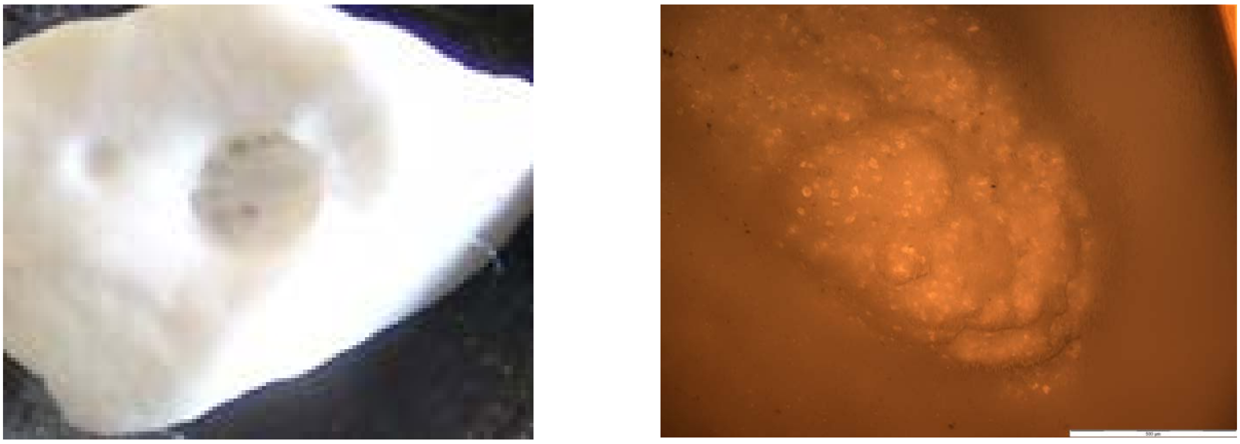

Figure 12. Laser ablated artificial stone material crater performed with thin disk Ho:YAG laser pulses of a few µs (left) and microscopic picture of a crater (right).

Summary:

A Ho:YAG thin disk laser is capable of delivering moderate high power laser pulses between 1 and 20 µs at repetition rates in the kHz-range with pulse energies of a few milli-Joule at an average output power in the order of 10 W which can be used in medical applications as a laser lithotripter. The ablation mechanism for the stone material (calcium oxalate monohydrate) is performed by a thermal decomposition of the stone into calcium carbonate starting at 400°C in combination with an additional much smaller ablation effect coming from the generated shock wave originating from the water vapor bubble implosion. The generation of the water vapor bubbles occurs in sequences between 50 to 100 ms depending on the single pulse energies and therefore on the average laser power. The period between single vapor bubbles can be separated into a heating phase of the water to create a vapor bubble and a heating phase of the stone material to the decomposition temperature. Compared to the state of the art lithotripter, the proposed laser lithotripter shows the advantage of a reduced optical damage of the fiber as well as a reduced surgical damage risk of nearby tissues in an actual laser surgery due to the low energies of the single laser pulses.

REFERENCES

[1] Vogel, A., ”Nonlinear absorption: intraocular microsurgery and laser lithotripsy”, Phys. Med. Biol. 42, 895-912 (1997).

[2] Rink, K., Delacretaz, G., and Salathe, R., ”Fragmentation process induced by microsecond laser pulses during lithotripsy”, Appl. Phys. Lett. 61 (3), 258-60 (1992).

[3] StarMedTec GmbH, innovative solutions, 82319 Starnberg, Germany.

[4] Pierre, S., Preminger, G., “Holmium laser for stone management”, World J. Urol. 25, 235-39 (2007).

[5] Scott, N., Cilip, Ch., and Fried, N., “Thulium fiber laser ablation of urinary stones through small-core optical fibers”, IEEE of Selected Topics in QE, vol. 15, no. 2, 435-40 (2009).

[6] Lamrini, S., Koopmann, Ph., Schäfer, M., Scholle, K., and Fuhrberg, P., “Directly diode-pumped high-energy Ho:YAG oscillator“, Optics Letters, vol. 37, no. 4, 1-3 (2012).

[7] Giesen, A., Hügel, H., Voss, A., Wittig, A., Brauch, U., and Opower, H., “Scalable concept for diode-pumped high power solid-sate lasers”, Appl. Phys. B 58, 365 (1994).

[8] Erhard, S., Giesen, A., Karzewski, M., Rupp, T., Steven, C., Johannsen, I., and Contag, K., “Novel pump design of Yb:YAG thin disk laser for operation at room temperature with improved efficiency “ , Advanced Solid State Lasers, Vol. 26, OSA Trends in Optics and Photonics, paper MC3 (1999).

[9] Shaw, L., Chang, R., and Djeu, N., “Measurement of up-conversion energy-transfer probabilities in Ho:YAG and Tm:YAG”, Physical Review B, Vol. 50, Nr. 10, 6609-6619 (1994).

[10] Rustad, G. and Stenersen, K., “Modeling of laser-pumped Tm and Ho lasers accounting for upconversion and ground-state depletion”, IEEE J. o. QE, vol. 21, no. 9, 1645-55 (1996).

[11] Barnes, N., Walsh, B., and Filer, E., “Ho:Ho upconversion: applications to Ho lasers”, J. Opt. Soc. Am. B Vol. 20, No. 6 June, 1212-19 (2003).

[12] Weiss, C. and Vilaseca, R., “Dynamics of Lasers”, VCH (1991).

[13] Dollimore, D., Tong, P., and Alexander, K., “The kinetic interpretation of the decomposition of calcium carbonate by use of relationships other than the Arrhenius equation”, Thermochimica Acta 282/283, 13-27 (1996).